ACS Infectious Diseases

pubs.acs.org/journal/aidcbc

Article

Boceprevir, Calpain Inhibitors II and XII, and GC-376 Have Broad-Spectrum Antiviral Activity against Coronaviruses

Yanmei Hu, Chunlong Ma, Tommy Szeto, Brett Hurst, Bart Tarbet, and Jun Wang*

Cite This: *ACS Infect. Dis.* 2021, 7, 586–597

Read Online

ACCESS | Metrics & More | Article Recommendations | Supporting Information

ABSTRACT: As the COVID-19 pandemic continues to unfold, the morbidity and mortality are increasing daily. Effective treatment for SARS-CoV-2 is urgently needed. We recently discovered four SARS-CoV-2 main protease (M^{pro}) inhibitors including boceprevir, calpain inhibitors II and XII, and GC-376 with potent antiviral activity against infectious SARS-CoV-2 in cell culture. In this study, we further characterized the mechanism of action of these four compounds using the SARS-CoV-2 pseudovirus neutralization assay. It was found that GC-376 and calpain inhibitors II and XII have a dual mechanism of action by inhibiting both viral M^{pro} and host cathepsin L in Vero cells. To rule out the cell-type dependent effect, the antiviral activity of these four compounds against SARS-CoV-2 was also confirmed in type 2 transmembrane serine protease-expressing Caco-2 cells using the viral yield reduction assay. In addition, we found that these four compounds have broad-spectrum antiviral activity in inhibiting not only SARS-CoV-2 but also SARS-CoV, and MERS-CoV, as well as human coronaviruses (CoVs) 229E, OC43, and NL63. The mechanism of action is through targeting the viral M^{pro}, which was supported by the thermal shift-binding assay and enzymatic fluorescence resonance energy transfer assay. We further showed that these four compounds have additive antiviral effect when combined with remdesivir. Altogether, these results suggest that boceprevir, calpain inhibitors II and XII, and GC-376 might be promising starting points for further development against existing human coronaviruses as well as future emerging CoVs.

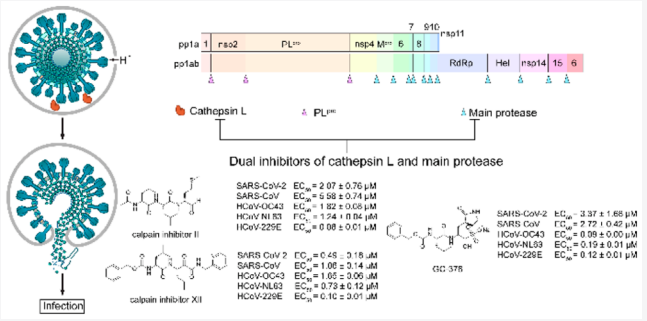

KEYWORDS: *SARS-CoV-2, COVID-19, main protease, boceprevir, GC-376, calpain inhibitor*

INTRODUCTION

Coronaviruses (CoVs) are enveloped positive-stranded RNA virus that infect humans and multiple species of animals, causing a variety of highly prevalent and severe diseases.[1] In the last two decades, three highly pathogenic and lethal human coronaviruses have emerged: severe acute respiratory syndrome coronavirus (SARS-CoV), the virus that caused the outbreak of severe acute respiratory syndrome in humans in Southern China in 2002 and killed 774 people among 8098 infected worldwide;[2] MERS-CoV, which caused severe respiratory disease outbreak in Middle East in 2012 and led to 791 deaths among 2229 infected;[3] the SARS-CoV-2, a novel coronavirus which emerged in China in December 2019, quickly spread worldwide, and became a global pandemic.[4] As of February 17, 2021, there have been more than 109 million confirmed cases and over 2.4 million deaths worldwide, and these numbers are increasing daily (https://coronavirus.jhu.edu/map.html). In addition, human coronavirus (HCoV) strains 229E (HCoV-229E), NL63 (HCoV-NL63), OC43 (HCoV-OC43), and HKU1 (HCoV-HKU1) cause a significant portion of the annual upper and lower respiratory tract infections in humans, including common colds, bronchiolitis, and pneumonia.[5−7] The current COVID-19 pandemic is a timely reminder of the urgent need for therapeutics against coronavirus infection. As future coronavirus outbreak cannot be excluded, broad-spectrum antivirals are desired to combat not only existing CoVs but also future emerging CoVs.

The coronavirus genome ranges from 26 to 32 kb, of which the 3′-terminal region, approximately one-third of the genome, encodes a number of structural proteins (spike protein, envelope protein, membrane protein, and nucleocapsid protein), while the 5′-terminal region, approximately two-thirds of the genome, encodes for the nonstructural proteins (3-chymotrypsin-like protease (3CL or main protease), papain-like protease, helicase, RNA-dependent RNA polymerase, exoribonuclease and endoribonuclease, methyl transferase), and accessary proteins.[8] Among the viral proteins under investigation as antiviral drug targets, the main protease (M^{pro}) appears to be a high-profile drug target for development

Received: October 28, 2020
Published: March 1, 2021

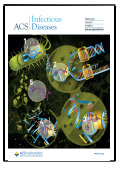

https://dx.doi.org/10.1021/acsinfecdis.0c00761
ACS Infect. Dis. 2021, 7, 586–597

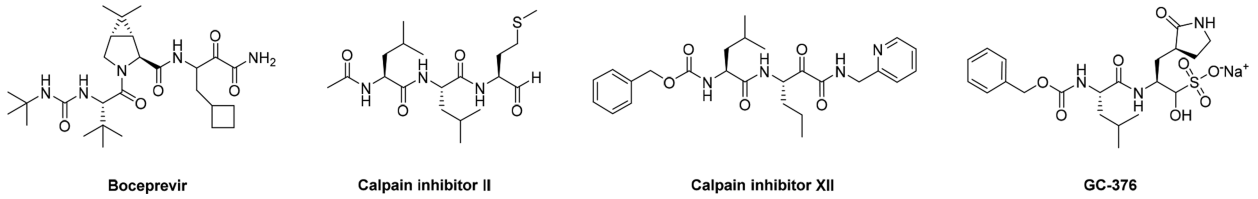

Figure 1. Chemical structures of SARS-CoV-2 M^{pro} inhibitors boceprevir, calpain inhibitors II and XII, and GC-376.

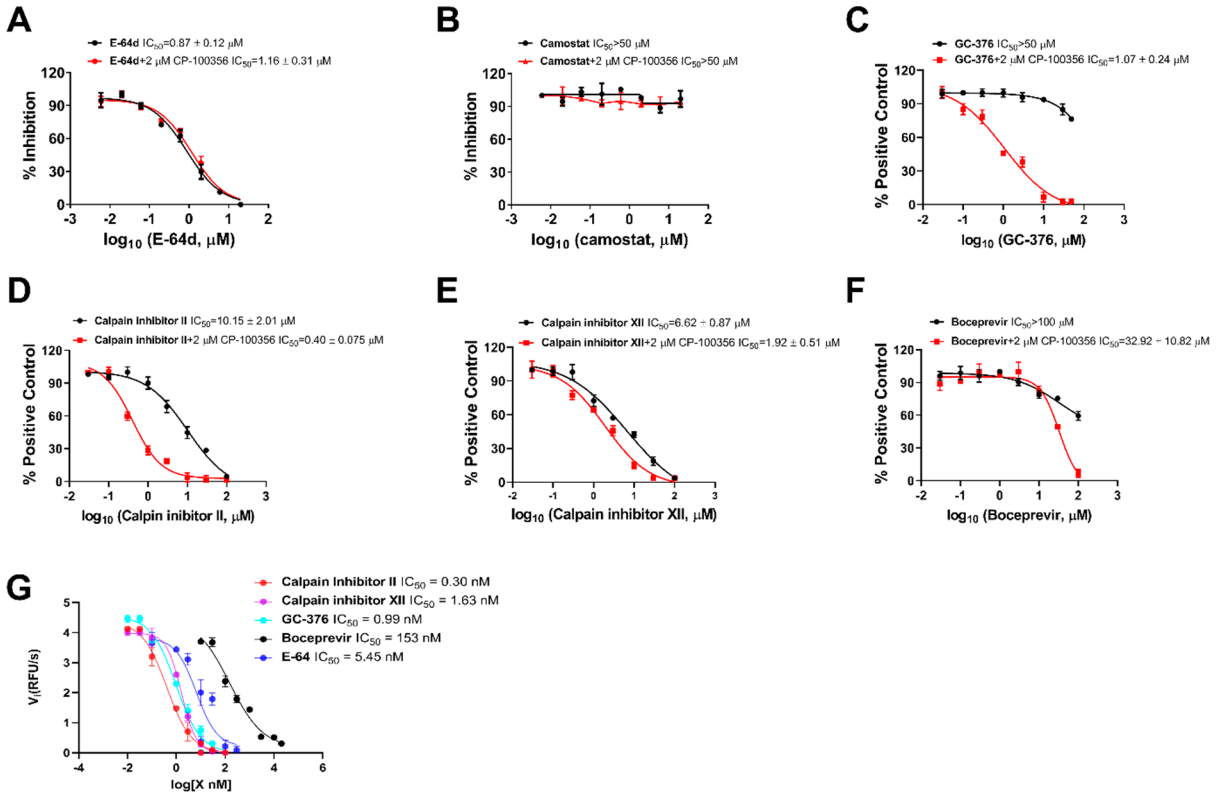

Figure 2. Inhibitory activity of GC-376, calpain inhibitors II and XII, and boceprevir in the SARS-CoV-2 pseudovirus neutralization assay. Effect of E-64d (A), camostat (B), GC-376 (C), calpain inhibitor II (D), calpain inhibitor XII (E), and boceprevir (F) on SARS-CoV-2 pseudovirus neuralization in the presence or absence of 2 μM P-gp inhibitor CP-100356. (G) Inhibition of cathepsin L in the FRET-based enzymatic assay. EC_{50} curve fittings using log (concentration of inhibitors) vs percentage of inhibition with variable slopes were performed in Prism 8. Data are mean ± standard deviation of two replicates.

of broad-spectrum antivirals for the following reasons: (1) M^{pro} plays an essential role in coronavirus replication by cleaving the viral polyproteins at more than 11 sites;[9] (2) M^{pro}s have relatively high sequence similarity within each CoV group;[10] (3) M^{pro} has an unique substrate preference for glutamine at the P1 site (Leu-Gln↓(Ser, Ala, Gly)), a feature that is absent in closely related host proteases,[11] suggesting it is feasible to design M^{pro} inhibitors with a high selectivity; (4) the structures of M^{pro}s from multiple members of the CoV family have been solved,[12−15] paving the way for rational drug design.

We recently discovered four SARS-CoV-2 M^{pro} inhibitors including boceprevir, calpain inhibitors II and XII, and GC-376 (Figure 1).[16] They had single-digit micromolar to submicromolar IC_{50} values in the enzymatic assay and inhibited SARS-CoV-2 viral replication in Vero cells with EC_{50} values in the single-digit micromolar to submicromolar range.[16] The cocrystal structures of GC-376, calpain inhibitors II and XII in complex with SARS-CoV-2 M^{pro} have been solved, providing a molecular explanation for the tight binding of these compounds toward M^{pro}.[16,17] We also found calpain inhibitors II and XII inhibit human cathepsin L in the *in vitro* enzymatic assay,[17] and cathepsin L has been shown to play an essential role in SARS-CoV-2 cell entry by activating the viral spike protein in the late endosome or lysosome.[18,19] A recent study also discovered that GC-373, the active form of GC-376, similarly inhibited the enzymatic activity of cathepsin L with an IC_{50} of 4.0 nM and showed cell-type dependent inhibition against SARS-CoV-2.[20] These observations led us to speculate that the cellular antiviral activity of calpain inhibitors II and XII, and GC-376 in Vero cells might be a result of inhibiting both viral M^{pro} and host cathepsin L. To test this hypothesis, we performed SARS-CoV-2 pseudovirus neutralization assay, and the results supported the contribution of inhibition of cathepsin L to the cellular antiviral activity of GC-376, and calpain inhibitors II and XII against SARS-CoV-2 in Vero cells.

SARS-CoV-2 enters the cell through two different pathways, either the type 2 transmembrane serine protease (TMPRSS2) mediated direct cell membrane fusion or endocytosis.[18,19] In the endocytosis pathway, endosome associated cathepsin L mediated the cleavage of viral spike protein and cathepsin L

https://dx.doi.org/10.1021/acsinfecdis.0c00761
ACS Infect. Dis. 2021, 7, 586−597

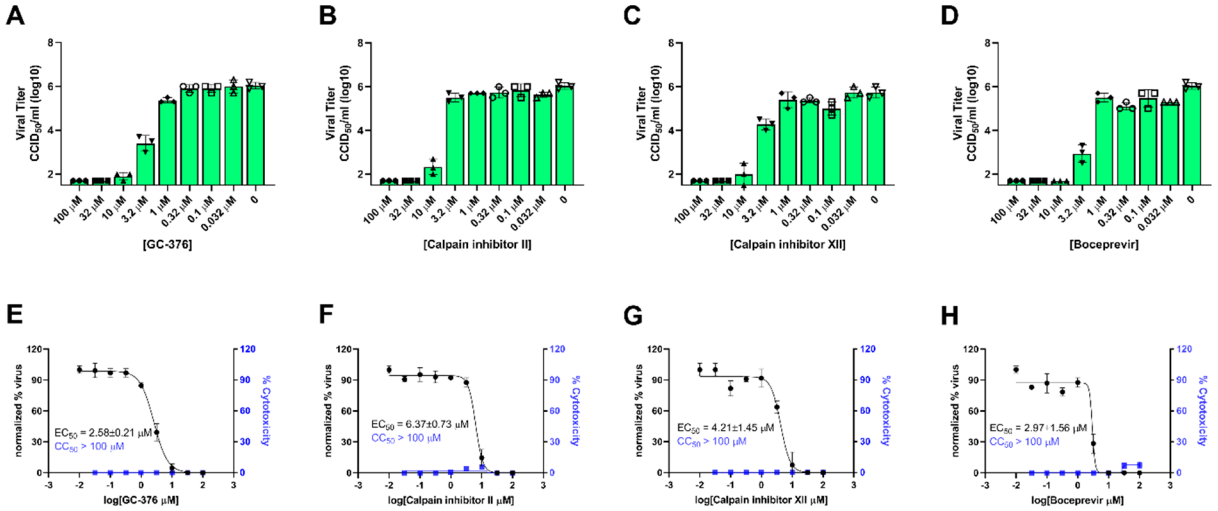

Figure 3. Viral yield reduction assay of SARS-CoV-2 in Caco-2 cells. (A–D) Raw data showing the SARS-CoV-2 viral titers in the presence of different concentrations of testing compounds. (E–H) Curve fitting for the antiviral EC_{50} values. Data are mean ± standard deviation of three independent replicates.

inhibitors have been shown to inhibit SARS-CoV-2 and SARS-CoV replication in cell culture.[18,19] However, the inhibition is cell-type dependent, and the antiviral activity is decreased or abolished in cells expressing TMRPSS2 that does not rely on endocytosis for viral entry.[18−20] To rule out the cell type dependent inhibition of these four compounds against SARS-CoV-2, we performed viral yield reduction (VYR) assay in Caco-2 cells, which expresses TMPRSS2 and is a physiological relevant cell culture model for SARS-CoV-2 replication,[19,21,22] and found that all four compounds had potent antiviral activity.

To evaluate the broad-spectrum antiviral activity of boceprevir, calpain inhibitors II and XII, and GC-376, we tested them against two other highly pathogenic coronaviruses, SARS-CoV and MERS-CoV, as well as three human coronaviruses HCoV-OC43, HCoV-NL63, and HCoV-229E. The mechanism of action was studied by the thermal shift-binding assay and fluorescence resonance energy transfer (FRET) based enzymatic assay. The combination therapy potential of these four compounds with remdesivir was also quantified by the drug combination index method. Altogether, our work demonstrated that boceprevir, calpain inhibitors II and XII, and GC-376 might be promising starting points for the design and development of broad-spectrum antivirals against current and future emerging CoVs.

RESULTS AND DISCUSSION

Calpain Inhibitors II and XII and GC-376, but Not Boceprevir, Inhibited SARS-CoV-2 Pseudovirus Neutralization in Vero Cells. Pseudovirus neutralization assay is an established model to study the mechanism of viral cell entry and has been widely used to assess the antiviral activity of viral entry/fusion and protease inhibitors.[23−25] Calpain inhibitors II and XII are potent inhibitors of human cathepsin L, with K_I and IC_{50} values in the nanomolar range.[17,26] Surprisingly, GC-376 was also shown to inhibit cathepsin L with an IC_{50} in the single-digit nanomolar range.[20] Cathepsin L plays an important role in SARS-CoV-2 viral entry by cleaving the viral spike S protein in the endosome or lysosome.[18,19] We therefore hypothesized that the cellular antiviral mechanism of calpain inhibitors II and XII and GC-376 in Vero cells might involve inhibition of cathepsin L besides M^{pro}. To test this hypothesis, we first generated SARS-CoV-2 pseudoviral particles in ACE2-expressing HEK293T cells (ACE2/293T) as previously described.[23] We then performed pseudovirus entry assay in Vero E6 cells, which have minimal levels of TMPRSS2 expression. As such, SARS-CoV-2 cell entry is mediated through endocytosis, which mainly relies on cathepsin L for viral spike protein activation.[18] E-64d, a known cathepsin L inhibitor, was included as a positive control. As Vero cells have high levels of efflux transporter P-glycoprotein (P-gp), which is also known as MDR1 and ABCB1,[27] the pseudovirus assay was performed with and without CP-100356, a P-gp efflux inhibitor. The purpose is to differentiate the effect of drug efflux from cathepsin L inhibition. It was found that the positive control E-64d was not a substrate of P-gp and inhibited SARS-CoV-2 pseudovirus entry in the presence or absence of CP-1000356 with similar potency (Figure 2A). The negative control, camostat, which is a TMPRSS2 inhibitor, did not inhibit SARS-CoV-2 pseudovirus entry with or without CP-100356 (Figure 2B). GC-376 did not inhibit SARS-CoV-2 pseudovirus entry in the absence of CP-100356 (IC_{50} > 50 μM) (Figure 2C black curve), contradictory to its potent inhibition of cathepsin L in the enzymatic assay as reported before.[20] It was known that the Pfizer clinical candidate PF-00835231 is a substrate of P-gp.[28] Given the structural similarity between PF-00835231 and GC-376, we hypothesized that GC-376 might also be a substrate of P-gp, and the lack of inhibition of GC-376 against the SARS-CoV-2 pseudovirus entry in Vero cells might be a result of drug efflux. Consistent with our hypothesis, it was found that GC-376 had potent inhibition of SARS-CoV-2 pseudovirus entry in the presence of CP-100356 with an IC_{50} of 1.07 ± 0.24 μM (Figure 2C red curve). This result suggests that the antiviral activity of GC-376 in Vero cells might involve the inhibition of cathepsin L. Both calpain inhibitors II and XII showed inhibitory activity against SARS-CoV-2 pseudovirus entry into Vero E6 cells with IC_{50} values of 10.15 ± 2.01 and 6.62 ± 0.87 μM, respectively, in the absence of CP-100356 (Figures 2D and E black curves). In the presence of CP-100356, calpain inhibitors II and XII showed more potent inhibition with IC_{50} values of 0.40 ± 0.08 and 1.92 ± 0.51 μM, respectively

https://dx.doi.org/10.1021/acsinfecdis.0c00761
ACS Infect. Dis. 2021, 7, 586−597

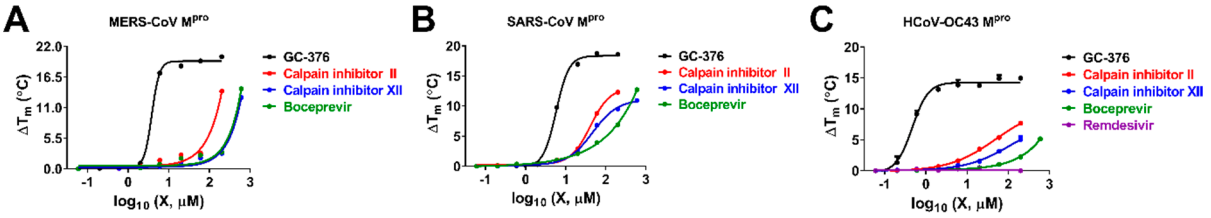

D

Compounds	MERS-CoV M^{pro} (ΔT_m, °C)	SARS-CoV M^{pro} (ΔT_m, °C)	HCoV-OC43 M^{pro} (ΔT_m, °C)
200 μM **remdesivir**	N.T.[a]	N.T.	0.00 ± 0.02
6 μM **GC-376**	17.23 ± 0.00	9.78 ± 0.07	13.86 ± 0.81
20 μM **calpain inhibitors II**	2.53 ± 0.28	2.88 ± 0.21	3.48 ± 0.02
20 μM **calpain inhibitors XII**	0.81 ± 0.14	2.41 ± 0.00	1.54 ± 0.01
60 μM **boceprevir**	2.46 ± 0.07	3.94 ± 0.13	1.02 ± 0.05

Figure 4. Effect of GC-376, calpain inhibitors II and XII, and boceprevir on melting temperature (T_m) of MERS-CoV M^{pro} (A), SARS-CoV M^{pro} (B), and HCoV-OC43 M^{pro} (C). Data were plotted with ΔT_m vs $\log_{10}$(concentrations of compound) using the Boltzmann Sigmoidal equation in Prism 8. Data are mean ± standard deviation of two replicates. (D) Melting temperature shift (ΔT_m) of MERS-CoV, SARS-CoV, and HCoV-OC43 M^{pro} in the presence of indicated concentrations of boceprevir, calpain inhibitors II and XII, and GC-376. [a]Not tested.

(Figures 2D and E red curves), suggesting both compounds are also P-gp substrates. In contrast, boceprevir had no effect on SARS-CoV-2 pseudovirus entry at up to 100 μM concentration (Figures 2F black curve) and showed weak inhibition in the presence of CP-100356 (IC_{50} = 32.92 ± 10.82 μM) (Figures 2F black curve). The enzymatic inhibition of GC-376, calpain inhibitors II and XII, and boceprevir on cathepsin L was tested using the FRET assay (Figure 2G). Consistent with previously enzymatic assay results as well as our SARS-CoV-2 pseudovirus neutralization assay results, calpain inhibitors II and XII and GC-376 had potent inhibition against cathepsin L with IC_{50}s ranging from 0.30 to 1.63 nM, similar to the positive control E-64 (IC_{50} = 5.45 nM), and boceprevir had weak inhibition with an IC_{50} of 153 nM. Altogether, it can be concluded that the cellular antiviral activity of GC-376, and calpain inhibitors II and XII in Vero cells involves the inhibition of cathepsin L, while boceprevir had little or no effect on cathepsin L-mediated viral entry. Our results also point out that the SARS-CoV-2 pseudovirus assay is a useful tool to evaluate the effect of drug candidates on the inhibition of cathepsin L as well as other host proteases that are involved in SARS-CoV-2 cell entry. With the P-gp inhibitor CP-100356, this assay can also identify compounds that might be P-gp substrates.

GC-376, Calpain Inhibitors II and XII, and Boceprevir Inhibited SARS-CoV-2 Replication in Caco-2 Cells Using Viral Yield Reduction (VYR) Assay. Given the dual inhibition mechanism of GC-376 and calpain inhibitors II and XII in inhibiting both cathepsin L and M^{pro}, it raised a potential concern of the potential cell type dependent inhibition for these compounds. As such, we further evaluated the antiviral potency of these four compounds against SARS-CoV-2 in Caco-2 cells. Caco-2 is a human colorectal adenocarcinoma cell line and has been shown to support the replication of SARS-CoV-2 at a similar level as the Calu-3 cell.[29−31] The Caco-2 cell line expresses TMPRSS2 and ACE2,[19,21,22] rendering it a physiologically relevant model for testing antiviral drug candidates. Using the viral yield reduction assay in Caco-2 cells, it was found that all four compounds GC-376, calpain inhibitors II and XII, and boceprevir inhibited SARS-CoV-2 replication with EC_{50} values of 2.58 ± 0.21, 6.37 ± 0.73, 4.21 ± 1.45, and 2.97 ± 1.56 μM, respectively (Figure 3). All four compounds were not toxic in Caco-2 cells (CC_{50} > 100 μM).

The potent antiviral activity of these three compounds against SARS-CoV-2 in Caco-2 cells suggest that although GC-376 and calpain inhibitors II and XII inhibit both host cathepsin L and viral M^{pro} in the in vitro enzymatic assay, cathepsin L inhibition appears to be dispensable and not essential for the antiviral activity, and M^{pro} inhibition might be the driving factor for their cellular antiviral activity. Nevertheless, we cannot rule out the possibility that these compounds might also inhibit other host proteases that are involved in viral replication.

Boceprevir, Calpain Inhibitors II and XII, and GC-376 Bind to MERS-CoV, SARS-CoV, and HCoV-OC43 M^{pro}. First, we performed sequence alignment of M^{pro} from multiple members of coronavirus family: HCoV-229E, HCoV-OC43, HCoV-NL63, SARS-CoV, MERS-CoV, and SARS-CoV-2 (Figure S1). Overall, the M^{pro}s showed moderate to high similarity in primary sequence and comparatively high sequence similarity within each CoV group (Figure S1). It is acknowledged that 3D structures of the M^{pro}s are more conserved, especially at the active site.[32] Therefore, we hypothesized that boceprevir, calpain inhibitors II and XII, and GC-376 might similarly bind to other CoV M^{pro}s in addition to SARS-CoV-2 M^{pro}. To test this hypothesis, we carried out differential scanning fluorimetry (DSF) assay.[33] Specific binding of a ligand to a protein typically stabilizes the target protein, resulting in an increased melting temperature (T_m). It was found that boceprevir, calpain inhibitors II and XII, and GC-376 increased the T_m of SARS-CoV, MERS-CoV, and HCoV-OC43 M^{pro} in a dose dependent manner (Figure 4), while remdesivir had no effect on HCoV-OC43 M^{pro} stability at up to 200 μM. This was expected as remdesivir is a known RNA-dependent RNA polymerase (RdRp) inhibitor.[34] GC-376 significantly increased the stability of all three M^{pro}s when tested at 6 μM, with ΔT_m of 17.23, 9.78, and 13.86

https://dx.doi.org/10.1021/acsinfecdis.0c00761
ACS Infect. Dis. 2021, 7, 586−597

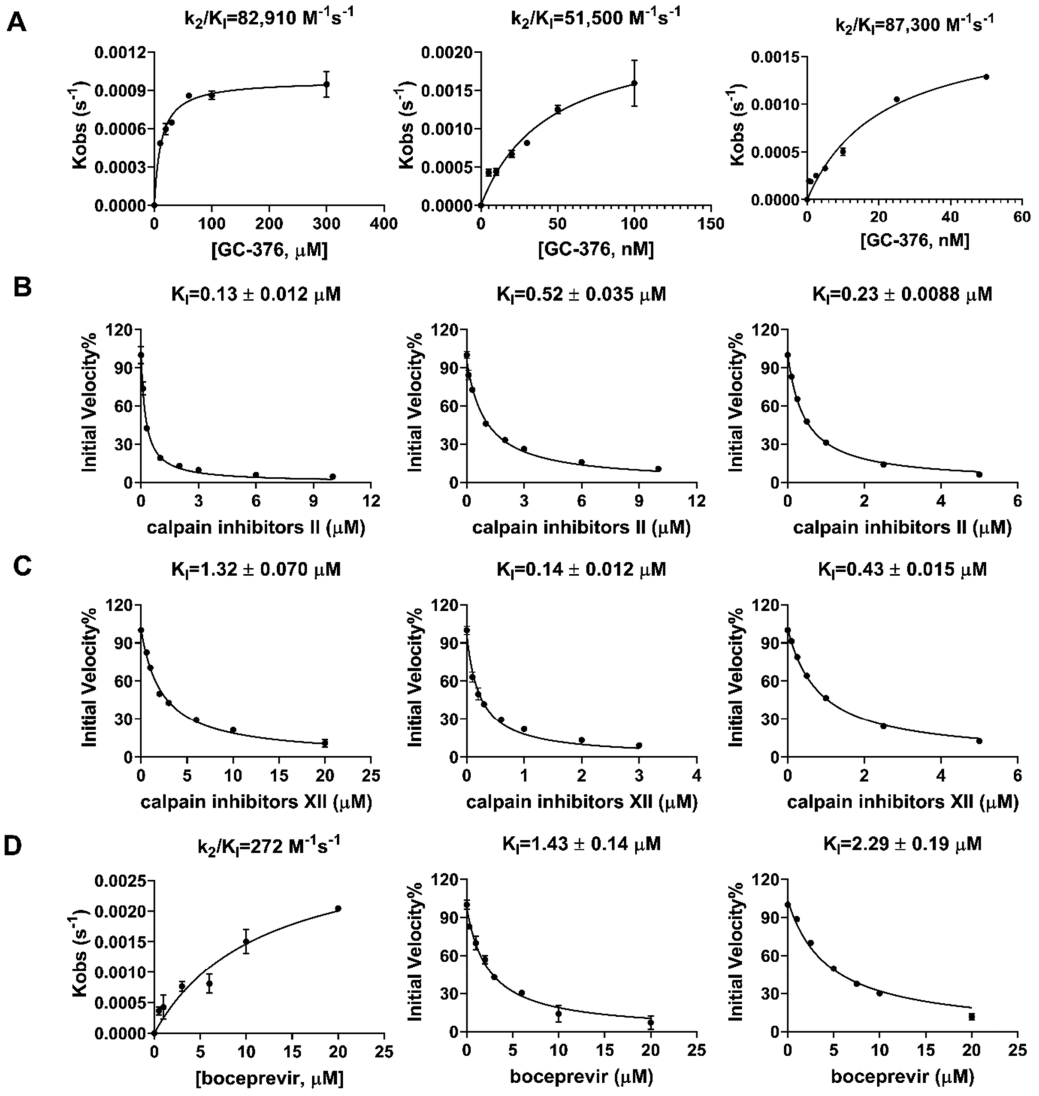

E

Compounds	SARS-CoV-2[a]	SARS-CoV	MERS-CoV	HCoV-OC43
GC-376	IC_{50}=0.030 ± 0.008 μM k_2/K_I = 40,800 $M^{-1}s^{-1}$	IC_{50}=0.079 ± 0.006 μM k_2/K_I =51,530 $M^{-1}s^{-1}$	IC_{50}=0.110 ± 0.023 μM k_2/K_I = 82,910 $M^{-1}s^{-1}$	IC_{50}=0.011 ± 0.0012 μM k_2/K_I =87,300 $M^{-1}s^{-1}$
Calpain inhibitor II	IC_{50}=0.97 ± 0.27 μM K_I = 0.40 μM	IC_{50}=2.04 ± 0.20 μM K_I = 0.60 μM	IC_{50}=1.24 ± 0.35 μM K_I = 0.13 μM	IC_{50}=0.56 ± 0.08 μM K_I =0.23 μM
Calpain Inhibitor XII	IC_{50}=0.45 ± 0.06 μM K_I = 0.13 μM	IC_{50}=0.60 ± 0.16 μM K_I = 0.14 μM	IC_{50}=6.68 ± 2.76 μM K_I = 1.32 μM	IC_{50}=0.34 ± 0.05 μM K_I =0.43 μM
Boceprevir	IC_{50}=4.13 ± 0.61 μM K_I = 1.18 μM	IC_{50}=6.63 ± 1.05 μM K_I = 1.43 μM	IC_{50}=10.41 ± 3.08 μM k_2/K_I = 272 $M^{-1}s^{-1}$	IC_{50}=9.0 ± 0.9 μM K_I =2.29 μM

Figure 5. Data fittings of the proteolytic reaction progression curves of MERS-CoV M^{pro} (left column), SARS-CoV M^{pro} (middle column), and HCoV-OC43 M^{pro} (right column) in the presence or the absence of GC-376 (A); calpain inhibitor II (B); calpain inhibitor III (C); and boceprevir (D). In the kinetic studies, 60 nM MERS-CoV M^{pro}, 5 nM SARS-CoV M^{pro}, or 3.3 nM HCoV-OC43 M^{pro} was added to a solution containing various concentrations of compounds and 20 μM FRET substrate to initiate the reaction. Detailed methods were described in the Methods section. Data are mean ± standard deviation of two replicates. (E) Enzymatic inhibition of boceprevir, calpain inhibitors II and XII, and GC-376 against various CoV M^{pro}s. [a]Data from ref 16.

°C against MERS-CoV, SARS-CoV, and HCoV-OC43 M^{pro}, respectively (Figure 4). Boceprevir and calpain inhibitors II and XII also stabilized all three M^{pro}s but were less potent than GC-376. Boceprevir increased the T_m of MERS-CoV, SARS-CoV, and HCoV-OC43 M^{pro} by 2.46, 3.94, and 1.02 °C, respectively at 60 μM (Figure 4). Calpain inhibitors II and XII increased the T_m of MERS-CoV, SARS-CoV, and HCoV-OC43 M^{pro} by 2.53, 2.88, 3.48 °C and 0.81, 2.41, 1.54 °C, respectively at 20 μM (Figure 4). This result confirmed that boceprevir, calpain inhibitors II and XII, and GC-376 had direct binding toward SARS-CoV, MERS-CoV, and HCoV-OC43 M^{pro}s in addition to SARS-CoV-2 M^{pro}, indicating they might be broad-spectrum antiviral drug candidates.

Boceprevir, Calpain Inhibitors II and XII, and GC-376 Inhibit the Enzymatic Activity of MERS-CoV, SARS-CoV, and HCoV-OC43 M^{pro}. To test whether boceprevir, calpain

https://dx.doi.org/10.1021/acsinfecdis.0c00761
ACS Infect. Dis. 2021, 7, 586−597

Table 1. Broad-Spectrum Antiviral Activity of Boceprevir, Calpain Inhibitors II and XII, and GC-376 against a Panel of Human CoVs in CPE Assay

compounds	HCoV-229E (EC_{50}, μM)	HCoV-NL63 (EC_{50}, μM)	HCoV-OC43 (EC_{50}, μM)	MERS-CoV (EC_{50}, μM)	SARS-CoV (EC_{50}, μM)	SARS-CoV-2[a] (EC_{50}, μM)
remdesivir	0.03 ± 0.00	0.63 ± 0.041	0.09 ± 0.00	NT[b]	NT	NT
GC-376	0.12 ± 0.01	0.19 ± 0.01	0.09 ± 0.00	0.83 ± 0.03	2.72 ± 0.42	3.37 ± 1.68
calpain inhibitor II	0.08 ± 0.01	1.24 ± 0.04	1.82 ± 0.08	5.48 ± 0.54	5.58 ± 0.74	2.07 ± 0.76
calpain inhibitor XII	0.10 ± 0.01	0.73 ± 0.12	1.65 ± 0.06	1.97 ± 0.10	1.06 ± 0.14	0.49 ± 0.18
boceprevir	14.12 ± 1.50	16.90 ± 5.87	16.84 ± 0.52	15.04 ± 0.63	54.17 ± 7.76	1.31 ± 0.58

[a]Data from ref 16. [b]Not tested.

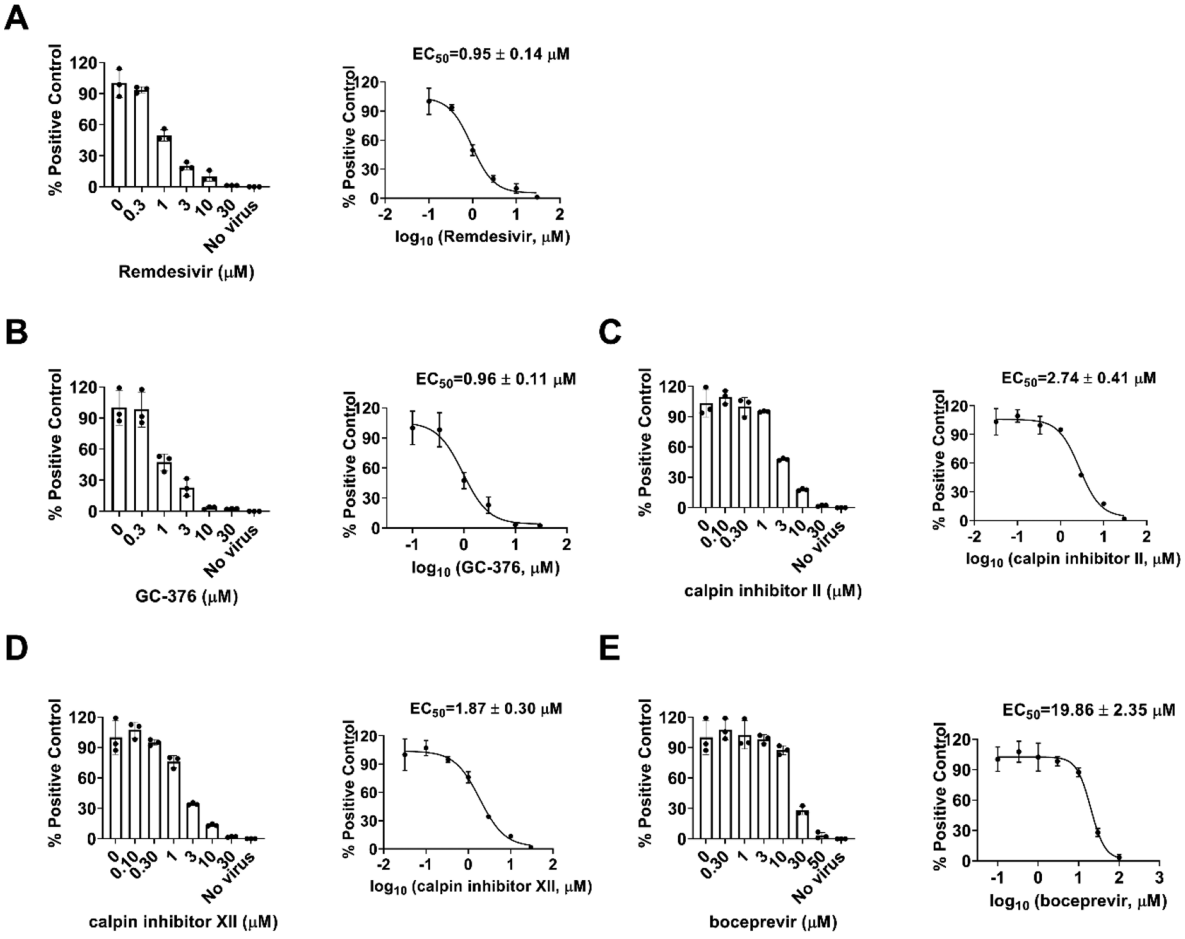

Figure 6. Dose-dependent inhibitory effect of GC-376, calpain inhibitors II and XII, and boceprevir on HCoV-NL63 viral RNA synthesis in Vero E6 cells using RT-qPCR assay. Positive control remdesivir (A); GC-376 (B); calpain inhibitor II (C); calpain inhibitor XII (D); and boceprevir (E). (left) Normalized RNA levels of the average of three repeats from each concentration tested and (right) EC_{50} curve fittings using log(concentration of inhibitors) vs normalized RNA levels with variable slopes in Prism 8. Data are mean ± standard deviation of three replicates.

inhibitors II and XII, and GC-376 inhibit the enzymatic activity of other CoV M^{pro}s, we performed enzyme kinetic studies of MERS-CoV, SARS-CoV, and HCoV-OC43 M^{pro} with different concentrations of these four compounds (Figure 5). The progression curves of all three CoV M^{pro} in the presence of different concentrations of GC-376 and MERS-CoV M^{pro} in the presence of different concentrations of boceprevir were fitted using the two-step reaction mechanism as previously described (Figures 5A–D).[16] In the first step, GC-376 binds to MERS-CoV, SARS-CoV, and HCoV-OC43 M^{pro} with an equilibrium dissociation constant (K_I) of 17.89 ± 2.34, 16.80 ± 2.36, and 3.63 ± 0.26 nM, respectively (Figure 5E). After initial binding, a covalent bond is formed at a slower velocity in the second step between GC-376 and the M^{pro}s with the second rate constant (k_2) being 1.48, 0.87, and 0.31 s^{-1}, respectively, resulting in an overall k_2/K_I value of 82 910, 51 500, and 87 300 M^{-1} s^{-1}, respectively (Figure 5A, E). Boceprevir binds to MERS-CoV M^{pro} with a K_I of 1.65 ± 0.12 μM in the first step and a k_2 of 448.8 s^{-1} in the second step, resulting in an overall k_2/K_I value of 272 M^{-1} s^{-1} (Figure 5D, E). When the proteolytic progression curves were fitted using the same two-step reaction mechanism, accurate values for the second rate constant k_2 could not be obtained for calpain inhibitors II and XII against all three M^{pro}s as well as boceprevir against SARS-CoV and HCoV-OC43 M^{pro}s. This is presumably due to significant substrate depletion before

https://dx.doi.org/10.1021/acsinfecdis.0c00761
ACS Infect. Dis. 2021, 7, 586–597

reaching the equilibrium between EI and EI*, leading to very small values of k_2. Therefore, only the dissociation constant K_I values from the first step were determined (Figure 5). The inhibition constants (K_I) for calpain inhibitors II and XII with respect to MERS-CoV, SARS-CoV, and HCoV-OC43 M^{pro} were 0.13 ± 0.012, 0.60 ± 0.041, and 0.23 ± 0.0088 μM and 1.32 ± 0.070, 0.14 ± 0.012, and 0.43 ± 0.015 μM, respectively; while the K_I values for boceprevir with respect to SARS-CoV and HCoV-OC43 M^{pro} were 1.43 ± 0.14 and 2.29 ± 0.19 μM, respectively. Taken together, the enzymatic kinetic results suggest that boceprevir, calpain inhibitors II and XII, and GC-376 have broad-spectrum enzymatic inhibition against SARS-CoV, MERS-CoV, and HCoV-OC43 M^{pro}.

Boceprevir, Calpain Inhibitors II and XII, and GC-376 Have Broad-Spectrum Antiviral Activity against Different CoVs. Given the binding and enzymatic inhibition of boceprevir, calpain inhibitors II and XII, and GC-376 against M^{pro} from multiple CoVs, we expect these compounds will have broad-spectrum antiviral activity against CoVs in cell culture. For this, cellular antiviral assays were performed against multiple human CoVs including HCoV-229E, HCoV-NL63, HCoV-OC43, MERS-CoV, and SARS-CoV. Remdesivir was included as a positive control. It was found that all four compounds showed potent antiviral activity against all the CoVs tested in the viral cytopathic effect (CPE) assay in a dose-dependent manner (Table 1 and Figure S3). The 50% effective concentration EC_{50} values of GC-376 range from 99 nM to 3.37 μM (Table 1 and Figure S3). Calpain inhibitors II and XII have comparable potency as GC-376, with EC_{50} values in the range of 84 nM to 5.58 μM and 100 nM to 1.97 μM, respectively (Table 1 and Figure S3). In contrast, boceprevir showed moderate antiviral activity against all the CoVs tested and the EC_{50} values were over 10 μM in most cases, except in the inhibition of SARS-CoV-2 (EC_{50} = 1.31 ± 0.58 μM) (Table 1). This result is in line with the weaker enzymatic inhibition of boceprevir against M^{pro}s compared with GC-376, calpain inhibitors II and XII (Figure 5E). Nevertheless, the lack of a linear correlation between the enzymatic inhibition (Figure 5E) and cellular antiviral activity (Table 1) might arise from several factors including membrane permeability, drug efflux, metabolism, and protein binding. Furthermore, the dual mechanism of action of GC-376 and calpain inhibitors II and XII in inhibiting viral M^{pro} and host cathepsin L further complicates the correlation.

To test whether boceprevir, calpain inhibitors II and XII, and GC-376 inhibit viral RNA synthesis, we performed the viral titer reduction assay using the RT-qPCR. HCoV-NL63 was chosen as a representative example and the viral nucleocapsid (N) gene expression level was detected in the absence or presence of different concentrations of compounds. Remdesivir was included as a positive control. All four compounds inhibited HCoV-NL63 viral N gene expression dose-dependently (Figure 7), giving EC_{50} values in the range of 0.96−19.86 μM (Figure 6), which were comparable to the EC_{50} values determined in the antiviral CPE assays (Table 1). Taken together, we have shown that boceprevir, calpain inhibitors II and XII, and GC-376 have broad-spectrum antiviral activity against CoVs.

Combination Therapy of Boceprevir, Calpain Inhibitors II and XII, and GC-376 with Remdesivir. The combination treatment potentials of boceprevir, calpain inhibitors II and XII, and GC-376 with remdesivir were explored using HCoV-OC43 antiviral CPE assay. Combination indices (CIs) versus the EC_{50} values of compounds at different combination ratios were plotted as previously described.[35] The red line indicates additive effect; the right upper area above the red line indicates antagonism, while the left bottom area below the line indicates synergy.[35] In all combination scenarios, the combination indices at all the combination ratios fell on the red line (Figure 7), suggesting that boceprevir, calpain inhibitors II and XII, and GC-376 displayed an additive antiviral effect with remdesivir in the combination therapy.

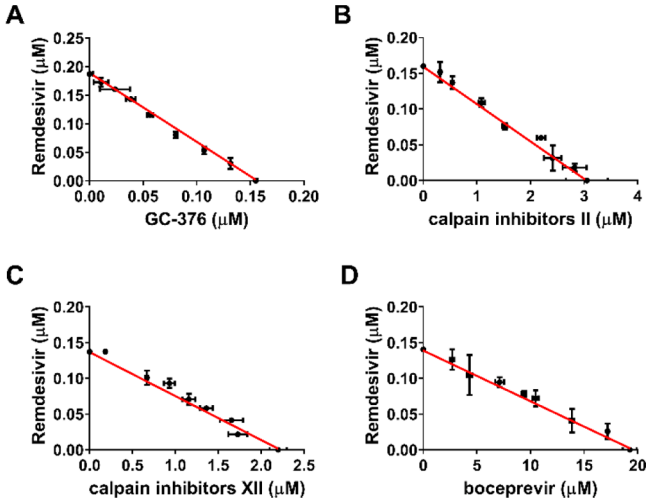

Figure 7. Combination therapy of remdesivir with GC-376 (A); calpain inhibitor II (B); calpain inhibitor XII (C); and boceprevir (D). Data are mean ± standard deviation of three replicates.

CONCLUSION

The COVID-19 pandemic that emerged in late December 2019 in China has had severe impacts on public health and the global economy. The high mortality rate and transmissibility of COVID-19 are unprecedented. There has been three outbreaks of highly pathogenic and lethal human coronaviruses within the past two decades,[2−4] and the current COVID-19 pandemic is a timely reminder of the urgent need for antivirals against CoVs. In this work, we report the broad-spectrum antiviral activity of our previously identified SARS-CoV-2 M^{pro} inhibitors boceprevir, calpain inhibitors II and XII, and GC-376 against multiple CoVs including the highly pathogenic SARS-CoV, MERS-CoV, and human coronaviruses NL63, 229E, and OC43. Coupled with their antiviral activity against SARS-CoV-2 as reported earlier, this result suggests that these four compounds might be promising starting points for the further development of broad-spectrum antivirals against not only current coronaviruses but also possibly future emerging coronaviruses. Among the four compounds, GC-376 and calpain inhibitors II and XII had a dual mechanism of action by targeting both the viral M^{pro} and host cathepsin L in Vero E6 cells. In this study, we provided additional evidence from pseudovirus neutralization assay to support this dual mechanism of action. We further demonstrated the additive antiviral effect of boceprevir, calpain inhibitors II and XII, and GC-376 with remdesivir in the combination therapy experiment. A recent study also showed the additive antiviral activity of GC-376 with remdesivir.[36]

It is known that CoVs enter host cells through two distinct pathways: the early membrane fusion pathway and the late

https://dx.doi.org/10.1021/acsinfecdis.0c00761
ACS Infect. Dis. 2021, 7, 586−597

endosomal pathway. For the early membrane fusion pathway, the TMPRSS2 is responsible for the viral spike protein cleavage and activation.[37] In the late endosomal entry pathway, the cysteine protease cathepsin L mediates the cleavage of spike protein.[18] Several CoVs including SARS-CoV-2, SARS-CoV, MERS-CoV, HCoV-OC43, HCoV-229E, and HCoV-NL63 utilize cathepsin L for host cell entry,[18,38−42] which offers an opportunity to develop broad-spectrum antivirals by targeting the cathepsin L protease. Indeed, cathepsin L inhibitors have been actively explored for the development of coronavirus antivirals.[43−45] However, the translational potential of cathepsin L inhibitors remains to be validated due to their cell-type dependent antviral effect.[18−20] No animal model studies have been conducted in evaluating the *in vivo* antiviral efficacy of cathepsin L inhibitors against SARS-CoV-2 infection. Given the dual mechanism of action of GC-376 and calpain inhibitors II and XII in inhibiting both M^{pro} and cathepsin L, there is a potential concern about cell-type dependent inhibition of these compounds. For this, we further tested the antiviral activity of these four compounds against SARS-CoV-2 in the TMPRSS2-expressing Caco-2 cells using viral yield reduction assay. It was found that all four compounds maintained potent antiviral activity, suggesting that the M^{pro} inhibition might be the predominant driving factor for the cellular antiviral activity. Inhibiting cathepsin L might be beneficial in TMPRSS2-negative cells but might not be essential in preventing viral infection in the lung.

Although M^{pro} is relatively conserved among coronaviruses and picornaviruses, not all $3CL^{pro}$ or $3C^{pro}$ inhibitors have broad-spectrum antiviral activity. For example, the well-known $3CL^{pro}$ inhibitor rupintrivir inhibits HCoV-229E with an EC_{50} value of 0.3 μM;[46] however it did not inhibit the M^{pro} from both SARS-CoV and SARS-CoV-2.[16,46] This might be due to the slight differences of residues located at the active sites of M^{pro}. Gratifyingly, we have shown in this study that boceprevir, calpain inhibitors II and XII, and GC-376 inhibited multiple M^{pro}s from different members of the coronavirus family and had potent cellular antiviral activity against all the coronaviruses tested. Among these four compounds, calpain inhibitors II and XII, and GC-376 had single-digit to submicromolar antiviral potency with a high selectivity index, while boceprevir had moderate to weak antiviral activity. Therefore, boceprevir might not be a viable drug candidate for repurposing in clinical trials. Nevertheless, boceprevir represents a novel chemotype that warrants the further development as a SARS-CoV-2 antiviral candidate. The cocrystal structure of SARS-CoV-2 M^{pro} with boceprevir has been solved and is expected to facilitate the structure−activity relationship studies.[36] It is important to highlight that the broad-spectrum antiviral activity of GC-376 and its analogs has been profiled.[46] In parallel to our study, GC-376 and calpain inhibitors II and XII were recently reported to inhibit HCoV-OC43 viral replication in cell culture,[47] which is consistent with our results. Moving forward, continuous optimization of boceprevir, calpain inhibitors II and XII, and GC-376 might yield clinical candidates with favorable pharmacokinetic properties and *in vivo* antiviral efficacy in animal models. Such studies are ongoing and will be reported when available.

METHODS

Cell Lines and Viruses. The following reagents were obtained through BEI Resources, NIAID, NIH: human embryonic kidney cells (HEK-293T) expressing human angiotensin-converting enzyme 2, HEK-293T-hACE2 cell line, NR-52511; SARS-related coronavirus 2, Wuhan-Hu-1 spike-pseudotyped lentiviral kit, NR-52948. Human rhabdomyosarcoma (RD), Vero E6, Huh-7, HEK293T expressing ACE2 (ACE2/293T), and HCT-8 cell lines were maintained in Dulbecco's modified eagle's medium (DMEM); Caco-2 and MRC-5 cell lines were maintained in eagle's minimum essential medium (EMEM). Both media were supplemented with 10% fetal bovine serum (FBS) and 1% penicillin-streptomycin antibiotics. Cells were kept at 37 °C incubator in a 5% CO_2 atmosphere. The following reagents were obtained through BEI Resources, NIAID, NIH: human coronavirus, OC43, NR-52725; human coronavirus, NL63, NR-470. HCoV-OC43 was propagated in RD cells; HCoV-NL63 was propagated in MRC-5 cells. HCoV-229E was obtained from Dr. Bart Tarbet (Utah State University) and amplified in Huh-7 or MRC-5 cells. The Urbani strain of severe acute respiratory syndrome coronavirus (SARS-CoV) and the EMC/2012 strain Middle East respiratory syndrome coronavirus (MERS-CoV) were obtained from the Centers for Disease Control and Prevention. Vero 76 cells were obtained from the American Type Culture Collection.

Pseudovirus Neutralization Assay. Pseudotype HIV-1-derived lentiviral particles bearing SARS-CoV-2 spike and a lentiviral backbone plasmid encoding luciferase as reporter was produced in HEK293 T cells engineered to express the SARS-CoV-2 receptor, ACE2 (ACE2/293 T cells), as previously described.[23] The pseudovirus was then used to infect Vero E6 cells in 96-well plates in the presence of DMSO or serial concentrations of E-64d, boceprevir, calpain inhibitors II and XII, and GC-376. At 48 hpi, cells from each well were lysed using the Bright-Glo Luciferase assay system (cat no.: E2610, Promega, Madison, WI, USA), and the cell lysates were transferred to 96-well Costar flat-bottom luminometer plates. The relative luciferase units (RLUs) in each well were detected using Cytation 5 cell imaging multi-mode reader (BioTek, Winooski, VT, USA).

Differential Scanning Fluorimetry (DSF). The binding of boceprevir, calpain inhibitors II and XII, and GC-376 to MERS-CoV, SARS-CoV, and HCoV-OC43 M^{pro}s was monitored by differential scanning fluorimetry (DSF) using a Thermal Fisher QuantStudio 5 Real-Time PCR System as previously described[48,49] with minor modifications. TSA plates were prepared by mixing M^{pro}s (final concentration of 4 μM) with different concentrations of compounds (0.2−200 μM) and incubated at 30 °C for 1 h. 1× SYPRO orange (Thermal Fisher) were added and the fluorescence signal was recorded under a temperature gradient ranging from 20 to 95 °C (incremental steps of 0.05 °C s^{-1}). The melting temperature (T_m) was calculated as the mid log of the transition phase from the native to the denatured protein using a Boltzmann model in Protein Thermal Shift Software v1.3. ΔT_m was calculated by subtracting reference melting temperature of proteins in the presence of DMSO from the T_m in the presence of compounds. Curve fitting was performed using the Boltzmann sigmoidal equation in Prism (v8) software.

Enzymatic Assays. For the measurements of K_M/V_{max} and IC_{50} values, proteolytic reactions were carried out with 100 nM MERS-CoV, SARS-CoV, or HCoV-OC43 M^{pro} in 100 μL of pH 6.5 reaction buffer (20 mM HEPES, pH 6.5, 120 mM NaCl, 0.4 mM EDTA, 4 mM DTT, and 20% glycerol) at 30 °C in a Cytation 5 imaging reader (Thermo Fisher Scientific) with filters for excitation at 360/40 nm and emission at 460/40 nm.

https://dx.doi.org/10.1021/acsinfecdis.0c00761
ACS Infect. Dis. 2021, 7, 586−597

Reactions were monitored every 90 s. For K_M/V_{max} measurements, a FRET substrate concentration ranging from 0 to 200 μM was applied. The initial velocity of the proteolytic activity was calculated by linear regression for the first 15 min of the kinetic progress curves. The initial velocity was plotted against the FRET concentration with the classic Michaelis−Menten equation in Prism 8 software. For IC_{50} measurements, 100 nM M^{pro} protein was incubated with 0.1 to 100 μM boceprevir, calpain inhibitors II and XII, and GC-376 at 30 °C for 30 min in reaction buffer, then the reaction was initiated by adding 10 μM FRET substrate. The reaction was monitored for 1 h, and the initial velocity was calculated for the first 15 min by linear regression. The IC_{50} was calculated by plotting the initial velocity against various concentrations of the compounds using a dose−response curve in Prism 8 software. Kinetics measurements of the proteolytic reaction progress curves with boceprevir, calpain inhibitors II and XII, and GC-376 were carried out as follows: 60 nM MERS-CoV M^{pro}, 5 nM SARS-CoV M^{pro}, or 3.3 nM HCoV-OC43 M^{pro} was added to 20 μM FRET substrate with various concentrations of compounds in 200 μL of reaction buffer at 30 °C to initiate the proteolytic reaction. The reaction was monitored for 4 h. The progress curves were fitted as previously described.[16] Substrate depletion was observed when proteolytic reactions progress longer than 90 min, therefore only the first 90 min of the progress curves were used in the curve fitting. In this study, k_2 for boceprevir, calpain inhibitors II and XII, could not be accurately determined because of significant substrate depletion before the establishment of the equilibrium between EI and EI*, leading to very slow k_2. In these cases, K_I was determined with Morrison equation in Prism 8.

SARS-CoV and MERS-CoV CPE Assays. Antiviral activities of test compounds were determined in nearly confluent cultures of Vero 76 cells. The assays were performed in 96-well Corning microplates. Cells were infected with approximately 30 cell culture infectious doses ($CCID_{50}$) of SARS-CoV or 40 $CCID_{50}$ of MERS-CoV. The plates were incubated at 37 °C with 5% CO_2 and 50% effective concentrations (EC_{50}) were calculated based on virus-induced cytopathic effects (CPE) quantified by neutral red dye uptake after 4 days of incubation for SARS-CoV or 3 days of incubation for MERS-CoV. Three microwells at each concentration of compound were infected. Two uninfected microwells served as toxicity controls. Cells were stained for viability for 2 h with neutral red (0.11% final concentration). Excess dye was rinsed from the cells with phosphate-buffered saline (PBS). The absorbed dye was eluted from the cells with 0.1 mL of 50% Sörensen's citrate buffer (pH 4.2)/50% ethanol. Plates were read for optical density determination at 540 nm. Readings were converted to the percentage of the results for the uninfected control using an Excel spreadsheet developed for this purpose. EC_{50} values were determined by plotting percent CPE versus log10 inhibitor concentration. Toxicity at each concentration was determined in uninfected wells in the same microplates by measuring dye uptake.

SARS-CoV-2 Viral Yield Reduction Assay in Caco-2 Cells. Caco-2 cells were maintained in MEM supplemented with 10% FBS. For antiviral assays, FBS reduced to 2% and the medium was supplemented with 50 μg mL^{-1} gentamicin. The test compounds were stored as 50 mM stocks in DMSO. The test compounds were prepared at eight serial half-log_{10} concentrations beginning at a high concentration of 100 μM.

Growth media was removed from the cells and the test compounds were applied to wells at 2× concentration. Virus at 400 $CCID_{50}$ (50% cell culture infectious dose) was added to the wells designated for virus infection corresponding to a multiplicity of infection (MOI) of 0.01. Plates were incubated at 37 °C with 5% CO_2 for 72 h. A sample of supernatant is taken from each infected well (three replicate wells pooled) and tested for virus titer determination.

Cytotoxicity was determined by the uptake of neutral red dye. Briefly, plates were stained with 0.011% neutral red for approximately two hours at 37 °C in a 5% CO_2 incubator. The neutral red medium was removed by aspiration, and the cells were rinsed 1× with phosphate buffered solution (PBS) to remove residual dye. The incorporated neutral red was eluted with 50% Sorensen's citrate buffer/50% ethanol for at least 30 min. The dye content in each well is quantified using a spectrophotometer at 540 nm wavelength. The dye content in each set of wells is converted to a percentage of dye present in untreated control wells using a Microsoft Excel computer-based spreadsheet and normalized based on the virus control. The 50% cytotoxic (CC_{50}, cell-inhibitory) concentrations are then calculated by regression analysis.

Titration of the viral samples (collected as described in the paragraph above) was performed by end point dilution.[50] Serial 1/10 dilutions of virus were prepared and plated into four replicate wells containing fresh cell monolayers of Vero 76 cells. Plates were then incubated, and cells are scored for the presence or absence of virus after distinct CPE is observed. The $CCID_{50}$ was calculated using the Reed−Muench method.[50] The 90% (one log_{10}) effective concentration (EC_{90}) is calculated by regression analysis by plotting the log_{10} of the inhibitor concentration versus log_{10} of virus produced at each concentration. The quotient of CC_{50} divided by EC_{90} gives the selectivity index (SI) value.

HCoV-OC43, HCoV-229E, and HCoV-NL63 CPE Assays. Antiviral activities of boceprevir, calpain inhibitors II and XII, and GC-376 against HCoV-229E, HCoV-NL63, and HCoV-OC43 were tested in CPE assays as previously described[51] with minor modifications. Briefly, cell cultures near confluency in 96-well plates were infected with 100 μL of viruses at desired dilutions and incubated for 1 h. Unabsorbed virus was removed and different concentrations of testing compounds (0, 0.01, 0.03, 0.1, 0.3, 1, 3, 10, 30, 100 μM) were added. Remdesivir was included as a positive control. The plates were incubated for another 3 to 5 days when a significant cytopathic effect was observed in the wells without compound (virus only). Cells were stained with 0.1 mg/mL neutral red for 2 h and excess dye was rinsed from the cells with PBS. The absorbed dye was dissolved with a buffer containing 50% ethanol and 1% glacial acetic acid. Plates were read for optical density determination at 540 nm. Readings were normalized with uninfected controls. EC_{50} values were determined by plotting percent CPE versus log_{10} compound concentrations from best-fit dose response curves with variable slope in Prism 8. Toxicity at each concentration was determined in uninfected cells in the same microplates by measuring neutral red dye uptake.

RNA Extraction and Real-Time PCR. RNA extraction and RT-PCR were performed as previously described.[52] Total RNA was extracted from HCoV-NL63 virus infected Caco-2 cells at an MOI of 0.05 at 48 h post infection using TRIzol reagents (Thermo Fisher Scientific). A 2.0 μg portion of total RNA was used to synthesize the first strand cDNA of viral

https://dx.doi.org/10.1021/acsinfecdis.0c00761
ACS Infect. Dis. 2021, 7, 586−597

RNA and host RNA using SuperScript III reverse transcriptase (Thermo Fisher Scientific) and Random Hexamer primer. Viral RNA was amplified on a Thermal Fisher QuantStudio 5 real-time PCR system (Thermo Fisher Scientific) using FastStart Universal SYBR Green Master mix (carboxy-X-rhodamine; Roche) and HCoV-NL63 N gene-specific primers (forward 5′-CTGTTACTTTGGCTTTAAAGAACTTAGG-3′; reverse 5′-CTCACTATCAAAGAATAACGCAGCCTG-3′). GAPDH was also amplified to serve as a control using human GAPDH-specific primers (GAPDH-F 5′-ACACCC-ACTCCTCCACCTTTG-3′; GAPDH-R 5′-CACCACCCTG-TTGCTGTAGCC-3′). The amplification conditions were as follows: 95 °C for 10 min; 40 cycles of 15 s at 95 °C and 60 s at 60 °C. Melting curve analysis was performed to verify the specificity of each amplification. All experiments were repeated three times independently.

Combination Therapy. Boceprevir, calpain inhibitors II and XII, and GC-376 was mixed with remdesivir at combination ratios of 8:1, 4:1, 2:1, 1:1, 1:2, 1:4, and 1:8 separately. The mixture of each compound with remdesivir at each combination ratio was serially diluted into seven different concentrations and applied in HCoV-OC43 CPE assay to determine EC_{50} of each compound and remdesivir in the combination ratio. A combination indices (CIs) plot was used to depict the EC_{50} values of each compound and remdesivir at different combination ratios. The red line indicates the additive effect; above the red line indicates the antagonism, while below the red line indicates the synergy.[35]

■ ASSOCIATED CONTENT

Supporting Information

The Supporting Information is available free of charge at https://pubs.acs.org/doi/10.1021/acsinfecdis.0c00761.

Sequence alignment of coronaviruses (Figure S1); amino acid conservation among HCoVs (Table S1); enzymatic kinetic studies of HCoV M^{pro}s in the presence or absence of inhibitors (Figure S2); cellular antiviral activity of GC-376, calpain inhibitors II and XII, and boceprevir against a panel of coronaviruses (Figure S3) (PDF)

■ AUTHOR INFORMATION

Corresponding Author

Jun Wang − *Department of Pharmacology and Toxicology, College of Pharmacy, The University of Arizona, Tucson, Arizona 85721, United States;* orcid.org/0000-0002-4845-4621; Phone: +1-520-626-1366; Email: junwang@pharmacy.arizona.edu

Authors

Yanmei Hu − *Department of Pharmacology and Toxicology, College of Pharmacy, The University of Arizona, Tucson, Arizona 85721, United States*

Chunlong Ma − *Department of Pharmacology and Toxicology, College of Pharmacy, The University of Arizona, Tucson, Arizona 85721, United States*

Tommy Szeto − *Department of Pharmacology and Toxicology, College of Pharmacy, The University of Arizona, Tucson, Arizona 85721, United States*

Brett Hurst − *Institute for Antiviral Research, Utah State University, Logan, Utah 84322, United States*

Bart Tarbet − *Institute for Antiviral Research, Utah State University, Logan, Utah 84322, United States*

Complete contact information is available at: https://pubs.acs.org/10.1021/acsinfecdis.0c00761

Author Contributions

Y.H., C.M., and J.W. designed the experiments. Y.H. performed the enzymatic assay, thermal shift binding assay, pseudovirus neutralization assay, antiviral assays against HCoV-OC43, HCoV-229E, and HCoV-NL63, and the combination therapy experiment. C.M. performed the enzymatic assays against SARS-CoV-2 M^{pro} and MERS-CoV M^{pro}. T.S. expressed and purified the SARS-CoV-2, SARS-CoV, and MERS-CoV M^{pro}. B.H. and B.T. performed the SARS-CoV and MERS-CoV CPE assays and the SARS-CoV-2 VYR assay in Caco-2 cells. Y.H. and J.W. wrote the manuscript with input from the others.

Notes

The authors declare the following competing financial interest(s): J.W. and C.M. are inventors of a pending patent that claimed the repurposing of boceprevir and GC-376 as SARS-CoV-2 antivirals.

■ ACKNOWLEDGMENTS

This research is supported by the NIH grants (AI119187, AI144887, AI147325, and AI157046) and the Young Investigator Award grant from the Arizona Biomedical Research Centre to J.W. (ADHS18-198859).

■ REFERENCES

(1) Hu, B., Guo, H., Zhou, P., and Shi, Z. L. (2021) Characteristics of SARS-CoV-2 and COVID-19. *Nat. Rev. Microbiol. 19*, 141.

(2) Hilgenfeld, R., and Peiris, M. (2013) From SARS to MERS: 10 years of research on highly pathogenic human coronaviruses. *Antiviral Res. 100*, 286−295.

(3) Zumla, A., Hui, D. S., and Perlman, S. (2015) Middle East respiratory syndrome. *Lancet 386*, 995−1007.

(4) Hui, D. S., I Azhar, E., Madani, T. A., Ntoumi, F., Kock, R., Dar, O., Ippolito, G., Mchugh, T. D., Memish, Z. A., Drosten, C., Zumla, A., and Petersen, E. (2020) The continuing 2019-nCoV epidemic threat of novel coronaviruses to global health - The latest 2019 novel coronavirus outbreak in Wuhan, China. *Int. J. Infect. Dis. 91*, 264−266.

(5) Cabeca, T. K., Granato, C., and Bellei, N. (2013) Epidemiological and clinical features of human coronavirus infections among different subsets of patients. *Influenza Other Respir. Viruses 7*, 1040−1047.

(6) van der Hoek, L., Pyrc, K., Jebbink, M. F., Vermeulen-Oost, W., Berkhout, R. J., Wolthers, K. C., Wertheim-van Dillen, P. M., Kaandorp, J., Spaargaren, J., and Berkhout, B. (2004) Identification of a new human coronavirus. *Nat. Med. 10*, 368−373.

(7) Woo, P. C., Lau, S. K., Chu, C. M., Chan, K. H., Tsoi, H. W., Huang, Y., Wong, B. H., Poon, R. W., Cai, J. J., Luk, W. K., Poon, L. L., Wong, S. S., Guan, Y., Peiris, J. S., and Yuen, K. Y. (2005) Characterization and complete genome sequence of a novel coronavirus, coronavirus HKU1, from patients with pneumonia. *J. Virol. 79*, 884−895.

(8) Su, S., Wong, G., Shi, W., Liu, J., Lai, A. C. K., Zhou, J., Liu, W., Bi, Y., and Gao, G. F. (2016) Epidemiology, Genetic Recombination, and Pathogenesis of Coronaviruses. *Trends Microbiol. 24*, 490−502.

(9) Anand, K., Ziebuhr, J., Wadhwani, P., Mesters, J. R., and Hilgenfeld, R. (2003) Coronavirus main proteinase (3CLpro) structure: basis for design of anti-SARS drugs. *Science 300*, 1763−1767.

(10) Khan, M. I., Khan, Z. A., Baig, M. H., Ahmad, I., Farouk, A. E., Song, Y. G., and Dong, J. J. (2020) Comparative genome analysis of

novel coronavirus (SARS-CoV-2) from different geographical locations and the effect of mutations on major target proteins: An in silico insight. *PLoS One 15*, e0238344.
(11) Chuck, C. P., Chow, H. F., Wan, D. C., and Wong, K. B. (2011) Profiling of substrate specificities of 3C-like proteases from group 1, 2a, 2b, and 3 coronaviruses. *PLoS One 6*, e27228.
(12) Zhang, L. L., Lin, D. Z., Sun, X. Y. Y., Curth, U., Drosten, C., Sauerhering, L., Becker, S., Rox, K., and Hilgenfeld, R. (2020) Crystal structure of SARS-CoV-2 main protease provides a basis for design of improved alpha-ketoamide inhibitors. *Science 368*, 409−412.
(13) Yang, H., Yang, M., Ding, Y., Liu, Y., Lou, Z., Zhou, Z., Sun, L., Mo, L., Ye, S., Pang, H., Gao, G. F., Anand, K., Bartlam, M., Hilgenfeld, R., and Rao, Z. (2003) The crystal structures of severe acute respiratory syndrome virus main protease and its complex with an inhibitor. *Proc. Natl. Acad. Sci. U. S. A. 100*, 13190−13195.
(14) Wang, F., Chen, C., Tan, W., Yang, K., and Yang, H. (2016) Structure of Main Protease from Human Coronavirus NL63: Insights for Wide Spectrum Anti-Coronavirus Drug Design. *Sci. Rep. 6*, 22677.
(15) Zhao, Q., Li, S., Xue, F., Zou, Y., Chen, C., Bartlam, M., and Rao, Z. (2008) Structure of the main protease from a global infectious human coronavirus, HCoV-HKU1. *J. Virol. 82*, 8647−8655.
(16) Ma, C., Sacco, M. D., Hurst, B., Townsend, J. A., Hu, Y., Szeto, T., Zhang, X., Tarbet, B., Marty, M. T., Chen, Y., and Wang, J. (2020) Boceprevir, GC-376, and calpain inhibitors II, XII inhibit SARS-CoV-2 viral replication by targeting the viral main protease. *Cell Res. 30*, 678−692.
(17) Sacco, M. D., Ma, C., Lagarias, P., Gao, A., Townsend, J. A., Meng, X., Dube, P., Zhang, X., Hu, Y., Kitamura, N., Hurst, B., Tarbet, B., Marty, M. T., Kolocouris, A., Xiang, Y., Chen, Y., and Wang, J. (2020) Structure and inhibition of the SARS-CoV-2 main protease reveals strategy for developing dual inhibitors against M(pro) and cathepsin L. *Sci. Adv. 6*, eabe0751.
(18) Shang, J., Wan, Y., Luo, C., Ye, G., Geng, Q., Auerbach, A., and Li, F. (2020) Cell entry mechanisms of SARS-CoV-2. *Proc. Natl. Acad. Sci. U. S. A. 117*, 11727−11734.
(19) Hoffmann, M., Kleine-Weber, H., Schroeder, S., Kruger, N., Herrler, T., Erichsen, S., Schiergens, T. S., Herrler, G., Wu, N. H., Nitsche, A., Muller, M. A., Drosten, C., and Pohlmann, S. (2020) SARS-CoV-2 Cell Entry Depends on ACE2 and TMPRSS2 and Is Blocked by a Clinically Proven Protease Inhibitor. *Cell 181*, 271.
(20) Steuten, K., Kim, H., Widen, J. C., Babin, B. M., Onguka, O., Lovell, S., Bolgi, O., Cerikan, B., Neufeldt, C. J., Cortese, M., Muir, R. K., Bennett, J. M., Geiss-Friedlander, R., Peters, C., Bartenschlager, R., and Bogyo, M. (2021) Challenges for Targeting SARS-CoV-2 Proteases as a Therapeutic Strategy for COVID-19. *ACS Infect. Dis.*, DOI: 10.1021/acsinfecdis.0c00815.
(21) Bertram, S., Glowacka, I., Blazejewska, P., Soilleux, E., Allen, P., Danisch, S., Steffen, I., Choi, S. Y., Park, Y., Schneider, H., Schughart, K., and Pohlmann, S. (2010) TMPRSS2 and TMPRSS4 facilitate trypsin-independent spread of influenza virus in Caco-2 cells. *J. Virol. 84*, 10016−10025.
(22) Stanifer, M. L., Kee, C., Cortese, M., Zumaran, C. M., Triana, S., Mukenhirn, M., Kraeusslich, H. G., Alexandrov, T., Bartenschlager, R., and Boulant, S. (2020) Critical Role of Type III Interferon in Controlling SARS-CoV-2 Infection in Human Intestinal Epithelial Cells. *Cell Rep. 32*, 107863.
(23) Crawford, K. H. D., Eguia, R., Dingens, A. S., Loes, A. N., Malone, K. D., Wolf, C. R., Chu, H. Y., Tortorici, M. A., Veesler, D., Murphy, M., Pettie, D., King, N. P., Balazs, A. B., and Bloom, J. D. (2020) Protocol and Reagents for Pseudotyping Lentiviral Particles with SARS-CoV-2 Spike Protein for Neutralization Assays. *Viruses 12*, 513.
(24) Nie, J., Li, Q., Wu, J., Zhao, C., Hao, H., Liu, H., Zhang, L., Nie, L., Qin, H., Wang, M., Lu, Q., Li, X., Sun, Q., Liu, J., Fan, C., Huang, W., Xu, M., and Wang, Y. (2020) Establishment and validation of a pseudovirus neutralization assay for SARS-CoV-2. *Emerging Microbes Infect. 9*, 680−686.
(25) Hu, Y., Meng, X., Zhang, F., Xiang, Y., and Wang, J. (2021) The in vitro antiviral activity of lactoferrin against common human coronaviruses and SARS-CoV-2 is mediated by targeting the heparan sulfate co-receptor. *Emerging Microbes Infect.*, 1.
(26) Sasaki, T., Kishi, M., Saito, M., Tanaka, T., Higuchi, N., Kominami, E., Katunuma, N., and Murachi, T. (1990) Inhibitory effect of di- and tripeptidyl aldehydes on calpains and cathepsins. *J. Enzyme Inhib. 3*, 195−201.
(27) De Rosa, M. F., Sillence, D., Ackerley, C., and Lingwood, C. (2004) Role of multiple drug resistance protein 1 in neutral but not acidic glycosphingolipid biosynthesis. *J. Biol. Chem. 279*, 7867−7876.
(28) Boras, B., Jones, R. M., Anson, B. J., Arenson, D., Aschenbrenner, L., Bakowski, M. A., Beutler, N., Binder, J., Chen, E., Eng, H., Hammond, J., Hoffman, R., Kadar, E. P., Kania, R., Kimoto, E., Kirkpatrick, M. G., Lanyon, L., Lendy, E. K., Lillis, J. R., Luthra, S. A., Ma, C., Noell, S., Obach, R. S., O'Brien, M. N., O'Connor, R., Ogilvie, K., Owen, D., Pettersson, M., Reese, M. R., Rogers, T., Rossulek, M. I., Sathish, J. G., Steppan, C., Ticehurst, M., Updyke, L. W., Zhu, Y., Wang, J., Chatterjee, A. K., Mesecar, A. D., Anderson, A. S., and Allerton, C. (2020) Discovery of a Novel Inhibitor of Coronavirus 3CL Protease as a Clinical Candidate for the Potential Treatment of COVID-19. *bioRxiv*, DOI: 10.1101/2020.09.12.293498.
(29) Chu, H., Chan, J. F., Yuen, T. T., Shuai, H., Yuan, S., Wang, Y., Hu, B., Yip, C. C., Tsang, J. O., Huang, X., Chai, Y., Yang, D., Hou, Y., Chik, K. K., Zhang, X., Fung, A. Y., Tsoi, H. W., Cai, J. P., Chan, W. M., Ip, J. D., Chu, A. W., Zhou, J., Lung, D. C., Kok, K. H., To, K. K., Tsang, O. T., Chan, K. H., and Yuen, K. Y. (2020) Comparative tropism, replication kinetics, and cell damage profiling of SARS-CoV-2 and SARS-CoV with implications for clinical manifestations, transmissibility, and laboratory studies of COVID-19: an observational study. *Lancet Microbe 1*, e14−e23.
(30) Bojkova, D., Klann, K., Koch, B., Widera, M., Krause, D., Ciesek, S., Cinatl, J., and Munch, C. (2020) Proteomics of SARS-CoV-2-infected host cells reveals therapy targets. *Nature 583*, 469−472.
(31) Lee, S., Yoon, G. Y., Myoung, J., Kim, S. J., and Ahn, D. G. (2020) Robust and persistent SARS-CoV-2 infection in the human intestinal brush border expressing cells. *Emerging Microbes Infect. 9*, 2169−2179.
(32) Ullrich, S., and Nitsche, C. (2020) The SARS-CoV-2 main protease as drug target. *Bioorg. Med. Chem. Lett. 30*, 127377.
(33) Niesen, F. H., Berglund, H., and Vedadi, M. (2007) The use of differential scanning fluorimetry to detect ligand interactions that promote protein stability. *Nat. Protoc. 2*, 2212−2221.
(34) Yin, W., Mao, C., Luan, X., Shen, D. D., Shen, Q., Su, H., Wang, X., Zhou, F., Zhao, W., Gao, M., Chang, S., Xie, Y. C., Tian, G., Jiang, H. W., Tao, S. C., Shen, J., Jiang, Y., Jiang, H., Xu, Y., Zhang, S., Zhang, Y., and Xu, H. E. (2020) Structural basis for inhibition of the RNA-dependent RNA polymerase from SARS-CoV-2 by remdesivir. *Science 368*, 1499−1504.
(35) Ma, C., Hu, Y., Zhang, J., and Wang, J. (2020) Pharmacological Characterization of the Mechanism of Action of RS23062, a Promising Antiviral for Enterovirus D68. *ACS Infect. Dis. 6*, 2260−2270.
(36) Fu, L., Ye, F., Feng, Y., Yu, F., Wang, Q., Wu, Y., Zhao, C., Sun, H., Huang, B., Niu, P., Song, H., Shi, Y., Li, X., Tan, W., Qi, J., and Gao, G. F. (2020) Both Boceprevir and GC376 efficaciously inhibit SARS-CoV-2 by targeting its main protease. *Nat. Commun. 11*, 4417.
(37) Bertram, S., Dijkman, R., Habjan, M., Heurich, A., Gierer, S., Glowacka, I., Welsch, K., Winkler, M., Schneider, H., Hofmann-Winkler, H., Thiel, V., and Pohlmann, S. (2013) TMPRSS2 activates the human coronavirus 229E for cathepsin-independent host cell entry and is expressed in viral target cells in the respiratory epithelium. *J. Virol. 87*, 6150−6160.
(38) Bosch, B. J., Bartelink, W., and Rottier, P. J. (2008) Cathepsin L functionally cleaves the severe acute respiratory syndrome coronavirus class I fusion protein upstream of rather than adjacent to the fusion peptide. *J. Virol. 82*, 8887−8890.

(39) Kawase, M., Shirato, K., Matsuyama, S., and Taguchi, F. (2009) Protease-mediated entry via the endosome of human coronavirus 229E. *J. Virol. 83*, 712−721.
(40) Park, J. E., Li, K., Barlan, A., Fehr, A. R., Perlman, S., McCray, P. B., Jr., and Gallagher, T. (2016) Proteolytic processing of Middle East respiratory syndrome coronavirus spikes expands virus tropism. *Proc. Natl. Acad. Sci. U. S. A. 113*, 12262−12267.
(41) Milewska, A., Nowak, P., Owczarek, K., Szczepanski, A., Zarebski, M., Hoang, A., Berniak, K., Wojarski, J., Zeglen, S., Baster, Z., Rajfur, Z., and Pyrc, K. (2018) Entry of Human Coronavirus NL63 into the Cell. *J. Virol. 92*, e01933−17.
(42) Owczarek, K., Szczepanski, A., Milewska, A., Baster, Z., Rajfur, Z., Sarna, M., and Pyrc, K. (2018) Early events during human coronavirus OC43 entry to the cell. *Sci. Rep. 8*, 7124.
(43) Simmons, G., Gosalia, D. N., Rennekamp, A. J., Reeves, J. D., Diamond, S. L., and Bates, P. (2005) Inhibitors of cathepsin L prevent severe acute respiratory syndrome coronavirus entry. *Proc. Natl. Acad. Sci. U. S. A. 102*, 11876−11881.
(44) Cannalire, R., Stefanelli, I., Cerchia, C., Beccari, A. R., Pelliccia, S., and Summa, V. (2020) SARS-CoV-2 Entry Inhibitors: Small Molecules and Peptides Targeting Virus or Host Cells. *Int. J. Mol. Sci. 21*, 5707.
(45) Liu, T., Luo, S., Libby, P., and Shi, G. P. (2020) Cathepsin L-selective inhibitors: A potentially promising treatment for COVID-19 patients. *Pharmacol. Ther. 213*, 107587.
(46) Kim, Y., Lovell, S., Tiew, K. C., Mandadapu, S. R., Alliston, K. R., Battaile, K. P., Groutas, W. C., and Chang, K. O. (2012) Broad-spectrum antivirals against 3C or 3C-like proteases of picornaviruses, noroviruses, and coronaviruses. *J. Virol. 86*, 11754−11762.
(47) Gurard-Levin, Z. A., Liu, C., Jekle, A., Jaisinghani, R., Ren, S., Vandyck, K., Jochmans, D., Leyssen, P., Neyts, J., Blatt, L. M., Beigelman, L., Symons, J. A., Raboisson, P., Scholle, M. D., and Deval, J. (2020) Evaluation of SARS-CoV-2 3C-like protease inhibitors using self-assembled monolayer desorption ionization mass spectrometry. *Antiviral Res. 182*, 104924.
(48) Musharrafieh, R., Ma, C., Zhang, J., Hu, Y., Diesing, J. M., Marty, M. T., and Wang, J. (2019) Validating Enterovirus D68−2A(pro) as an Antiviral Drug Target and the Discovery of Telaprevir as a Potent D68−2A(pro) Inhibitor. *J. Virol. 93*, e02221−02218.
(49) Ma, C., and Wang, J. (2021) Dipyridamole, chloroquine, montelukast sodium, candesartan, oxytetracycline, and atazanavir are not SARS-CoV-2 main protease inhibitors. *Proc. Natl. Acad. Sci. U. S. A. 118*, e2024420118.
(50) Reed, L. J., and Muench, H. (1938) A simple method of estimating fifty percent endpoints. *Am. J. Epidemiol. 27*, 493−498.
(51) Hu, Y., Zhang, J., Musharrafieh, R. G., Ma, C., Hau, R., and Wang, J. (2017) Discovery of dapivirine, a nonnucleoside HIV-1 reverse transcriptase inhibitor, as a broad-spectrum antiviral against both influenza A and B viruses. *Antiviral Res. 145*, 103−113.
(52) Zhang, J., Hu, Y., Foley, C., Wang, Y., Musharrafieh, R., Xu, S., Zhang, Y., Ma, C., Hulme, C., and Wang, J. (2018) Exploring Ugi-Azide Four-Component Reaction Products for Broad-Spectrum Influenza Antivirals with a High Genetic Barrier to Drug Resistance. *Sci. Rep. 8*, 4653.

https://dx.doi.org/10.1021/acsinfecdis.0c00761
ACS Infect. Dis. 2021, 7, 586−597